Molecular Determinants for DNA Minor Groove Recognition: Design of a Bis-Guanidinium Derivative of Ethidium That Is Highly Selective for AT-Rich DNA Sequences†

Christian Bailly,*,‡ Reem K. Arafa,§ Farial A. Tanious,§ William Laine,‡ Christèle Tardy,‡ Amélie Lansiaux,‡ Pierre Colson,|| David W. Boykin,*,§ and W. David Wilson*,§

INSERM U-524 et Laboratoire de Pharmacologie Antitumorale du Centre Oscar Lambret, IRCL, 59045 Lille, France, Biospectroscopy and Physical Chemistry Unit, Department of Chemistry and Natural and Synthetic Drugs Research Center, University of Liege, Sart-Tilman, 4000 Liege, Belgium, and Department of Chemistry and Laboratory for Chemical and Biological Sciences, Georgia State University, Atlanta, Georgia 30303

Received September 19, 2004; Revised Manuscript Received November 24, 2004

ABSTRACT: The phenanthridinium dye ethidium bromide is a prototypical DNA intercalating agent. For decades, this anti-trypanosomal agent has been known to intercalate into nucleic acids, with little preference for particular sequences. Only polydA-polydT tracts are relatively refractory to ethidium intercalation. In an effort to tune the sequence selectivity of known DNA binding agents, we report here the synthesis and detailed characterization of the mode of binding to DNA of a novel ethidium derivative possessing two guanidinium groups at positions 3 and 8. This compound, DB950, binds to DNA much more tightly than ethidium and exhibits distinct DNA-dependent absorption and fluorescence properties. The study of the mode of binding to DNA by means of circular and electric linear dichroism revealed that, unlike ethidium, DB950 forms minor groove complexes with AT sequences. Accurate quantification of binding affinities by surface plasmon resonance using A_nT_n hairpin oligomer indicated that the interaction of DB950 is over 10−50 times stronger than that of ethidium and comparable to that of the known minor groove binder furamidine. DB950 interacts weakly with GC sites by intercalation. DNase I footprinting experiments performed with different DNA fragments established that DB950 presents a pronounced selectivity for AT-rich sites, identical with that of furamidine. The replacement of the amino groups of ethidium with guanidinium groups has resulted in a marked gain of both affinity and sequence selectivity. DB950 provides protection against DNase I cleavage at AT-containing sites which frequently correspond to regions of enhanced cleavage in the presence of ethidium. Although DB950 maintains a planar phenanthridinium chromophore, the compound no longer intercalates at AT sites. The guanidinium groups of DB950, just like the amidinium group of furamidine (DB75), are the critical determinants for recognition of AT binding sites in DNA. The chemical modulation of the ethidium exocyclic amines is a profitable option to tune the nucleic acid recognition properties of phenylphenanthridinium dyes.

For decades *molecular entrepreneurs* in academic and pharmaceutical laboratories have sought methods to design and develop nucleic acid targeted drugs (*1*, *2*). The quest of chemists, biophysicists, and pharmacologists for small molecules capable of targeting key DNA sequences has led to the development of several classes of genome-targeted compounds of potential therapeutic interest, for the treatment of various human illnesses: mainly cancer, parasitic diseases, and viral infections (*3*−*5*). The study and description of DNA binding drugs was initiated in the early 1960s, soon after the disclosure of the Watson−Crick double-helix DNA structure, with the pioneer characterization of the DNA intercalation model followed by the DNA minor groove binding model in the 1970s (*6*−*9*). The initial view that planar aromatic molecules, such as acridines and ellipticines, for example, essentially provide DNA intercalating agents that insert between two consecutive base pairs of the double helix remains a solid concept. However, atypical DNA intercalating agents lacking a planar aromatic chromophore are not rare species and there have been frequent surprises with nonplanar, noncondensed molecules that are a priori inadequately shaped for intercalation but which have been found to be excellent intercalating agents. Such examples include the diuretic drug amiloride (*10*, *11*) and certain triphenyl methane dyes such as crystal violet (*12*).

In contrast, there is a common view that minor groove binders generally exhibit an extended, crescent-shaped

† This work was supported by grants (to C.B.) from the Ligue Nationale Contre le Cancer (Comité du Nord) and the Institut de Recherches sur le Cancer de Lille and (to W.D.W. and D.W.B.) from the National Institutes of Health (NIH Grant No. GM61587), the Georgia Research Alliance, and a Gates Foundation grant. Support by the "Actions intégrées Franco-Belge, Program Tournesol" is acknowledged. This work is dedicated to the memory of Professor Claude Hélène (deceased Feb 11, 2003).

* To whom correspondence should be addressed. E-mail: christian.bailly@lille.inserm.fr (C.B.); chedwb@panther.gsu.edu (D.W.B.); chewdw@panther.gsu.edu (W.D.W.). Tel: +33 320 16 92 20 (C.B.). Fax: +33 320 16 92 29) (C.B.).

‡ INSERM U-524.

§ Georgia State University.

|| University of Liege.

10.1021/bi047983n CCC: $30.25
Published on Web 01/15/2005

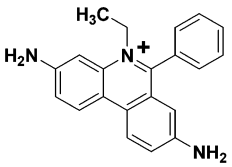

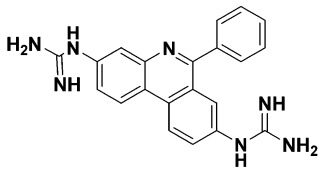

FIGURE 1: Structures of the compounds described in this study.

skeleton complementary to a spiral portion of the DNA helical structure. Here again, while this idea is broadly correct, there are examples of molecules that do not present this general extended architecture but effectively fit into the minor groove of DNA. In all cases, subtle modifications of the structure of a given DNA ligand can have a profound impact on its binding mode that also depends on the sequence and structure of the target DNA receptor site.

A typical example of sequence-dependent binding mode to DNA was initially reported with the antiparasitic drug DAPI, a diamidinophenylindole derivative which binds tightly to the minor groove of AT-rich DNA sequences and intercalates at GC sites (*13*, *14*). Different unfused aromatic dications such as the compounds berenil and Hoechst 33258 have shown similar properties: minor groove binding at AT sites and intercalation at GC sites (*15*). In these cases, it is the sequence and structure of the DNA binding sites which dictate the mode of binding of the ligand. In contrast, it is sometimes possible to adapt the structure of the ligand so as to modulate its DNA recognition properties. One of the best examples is the drug furamidine (DB75, Figure 1), a highly potent AT-specific minor groove binder that can be converted into a GC-selective intercalating agent by replacing its two terminal amidine functions by imidazoline groups. These structural variations not only affect the mode of binding to DNA but they also have a profound impact on the pharmacological properties of these drugs. Furamidine is a potent anti-parasitic agent, and an amidoxime prodrug of DB75 (DB289, *16*) is currently undergoing phase II clinical trials for the treatment of African trypanosomiasis, *Pneumocystis carinii* pneumonia, and malaria, whereas furimidazoline (DB60) is a cytotoxic agent (*17*). The marked activity of DB60 against cisplatin-resistant cell lines makes this drug a potential lead compound for the development of antitumor agents (*18*). These examples, and several others, indicate that the manipulation of the DNA binding properties of a drug is an option to control its therapeutic activity.

One of the most frequently used and well characterized DNA intercalating agents is the phenanthridine dye ethidium bromide (Figure 1). Forty years ago, this compound served to seal the hydrodynamic basis of the DNA intercalation model and contributed to the measure of DNA supercoiling (*19*−*22*). Over the past four decades, its DNA/RNA intercalative binding properties have been thoroughly investigated by a multitude of techniques, including X-ray diffraction (*23*, *24*), fluorescence (*25*−*27*), NMR (*28*−*31*), spectrophotometry (*32*), equilibrium dialysis (*33*−*35*), stopped-flow (*36*), calorimetry (*37*−*40*), polarimetric (*41*) and electrooptical methods (*42*, *43*), linear dichroism (*44*, *45*), molecular modeling (*46*), DNase I footprinting (*47*), photoaffinity (*48*, *49*), chemical cross-linking (*50*), topoisomerase-based assays (*51*), and many other gel-based and physicochemical and spectroscopic methods.

Half a century after the first synthesis of ethidium bromide (*52*), this purple compound remains the most extensively employed dye in molecular biology to stain nucleic acids in gels and to study a panoply of nucleic acid structures: DNA triplexes (*53*−*56*), Z-to-B DNA transition (*57*, *58*), DNA branches (*34*), bulges in RNA and DNA (*59*, *60*), and chromatin structures (*61*, *62*), for example. Ethidium continues to serve as a lead structure for the design of drugs targeting specific nucleic acid structures, such as DNA quadruplexes (*63*, *64*) and bulges in RNA (*65*), for example. Ethidium has also been exploited to construct hybrid molecules for tight and/or sequence-selective binding to DNA and RNA (*66*−*71*). One of the main reasons for the extensive use of this compound as a lead for nucleic acid recognition is its fluorescence, which is considerably enhanced upon binding to DNA or RNA (as a result of a reduction in the rate of excited-state proton transfer to solvent molecules (*72*)), thus providing a convenient and facile detection system.

In terms of pharmacology, ethidium was initially reported as a potent inhibitor of nucleic acid synthesis (*73*) and this activity likely accounts for its antibacterial and antitrypanocidal properties (*74*). Despite its recognized mutagenic activity (*75*), ethidium bromide remains used for the treatment of animal trypanosomiasis in Africa (*76*).

In the course of a medicinal chemistry program aimed at designing noncarcinogenic phenanthridine derivatives, a bisguanidinium derivative of ethidium designated DB950 (Figure 1) was synthesized. We report here its synthesis and DNA binding properties studied using a range of complementary spectroscopic and biochemical methods to determine its affinity for duplex DNA, mode of binding, and sequence selectivity. The discovery that DB950 forms stable minor groove complexes preferentially at AT-rich sequences in DNA provides a novel example of modulation of the mechanism of binding a drug to DNA. The conversion of the well-known DNA intercalating agent ethidium bromide into a minor groove binder by virtue of an amine → guanidine substitution may provide an interesting strategy to optimize the targeting of DNA sequences by small molecules.

MATERIALS AND METHODS

Chemistry. Melting points were recorded using a Mel-Temp 3.0 capillary melting point apparatus and are uncorrected. TLC analysis was carried out on silica gel 60 F_{254} precoated aluminum sheets and detected under UV light. ^{1}H and ^{13}C NMR spectra were recorded employing a Varian GX400 or Varian Unity Plus 300 spectrometer, and chemical

shifts (δ) are in ppm relative to TMS as internal standard. Mass spectra were recorded on a VG Analytical 70-SE spectrometer at the Georgia Institute of Technology, Atlanta, GA. Elemental analyses were obtained from Atlantic Microlab Inc. (Norcross, GA). All chemicals and solvents (including anhydrous solvents) were purchased from Aldrich Chemical Co. or Fisher Scientific and used as purchased. Triethylamine (CaH_2) was distilled from the indicated drying agent.

Preparation of 3,8-Bis(N′,N″-di-BOCguanidino)-6-phenylphenanthridine (**2**). To a solution of 3,8-diamino-6-phenylphenanthridine (**1**; 0.50 g, 1.8 mmol) and 1,3-bis(*tert*-butoxycarbonyl)-2-methyl-2-thiopseudourea (1.08 g, 3.7 mmol) in anhydrous DMF (15 mL) was added triethylamine (1.11 g, 11.0 mmol) and mercury(II) chloride (1.10 g, 4.1 mmol), simultaneously. The resulting suspension was stirred at room temperature for 24 h. The reaction mixture was diluted with CH_2Cl_2, Na_2CO_3 solution was added, and the mixture was filtered through a pad of Celite. The organic layer was washed with water (3×) and then brine. After drying over anhydrous Na_2SO_4, the solvent was evaporated to dryness under reduced pressure and the residue obtained was purified by column chromatography using hexane−EtOAc−CH_2Cl_2 (80:10:10) as eluent to give tan white flaky crystals (0.9 g, 67%), mp >400 °C. ^{1}H NMR ($CDCl_3$): δ 1.50, 1.53 (2s, 36H), 7.51−7.60 (m, 3H), 7.77 (dd, J = 8.7, 1.8 Hz, 2H), 8.01 (t, J = 8.7 Hz, 2H), 8.34 (d, J = 1.8 Hz, 1H), 8.40 (d, J = 1.8 Hz, 1H), 8.49 (d, J = 8.7 Hz, 1H), 8.57 (d, J = 8.7 Hz, 1H), 10.43 (br s, 1H), 10.66 (br s, 1H), 11.62 (br s, 1H), 11.69 (br s, 1H). ^{13}C NMR ($CDCl_3$): δ 163.6, 161.3, 153.6, 144.0, 139.5, 137.1, 135.1, 130.4, 129.8, 128.7, 128.4, 126.1, 125.2, 122.8, 122.5, 122.1, 122.0, 121.6, 120.5, 83.9, 79.7, 28.1. MS (ESI): *m*/*z* 770.4 ($M^+ + 1$), 670.3, 570.3, 354.1, 338.3, 273.6 (100%). Anal. Calcd for $C_{41}H_{51}N_7O_8$ (769.88): C, 63.96; H, 6.67; N, 12.73. Found: C, 63.97; H, 6.83; N, 12.58.

Deprotection of N′,N″-Di-BOCguanidine. 3,8-Bis(guanidino)-6-phenyl-phenanthridine Trihydrochloride (**3**). A chilled solution of the *tetra*-BOCguanidine (**2**; 0.40 g, 0.5 mmol) in CH_2Cl_2 (10 mL), diluted with dry EtOH (5 mL), was saturated with anhydrous HCl. The reaction mixture was stirred at room temperature for 3 days, with precipitate forming over time indicating product formation (shorter reaction time gives incomplete deprotection). The solvent was then evaporated to dryness, the residue washed with ether, and the salt left to dry under vacuum at 50 °C overnight to give a greenish solid (0.26 g), mp 277−279 °C. ^{1}H NMR (DMSO-d_6): δ 7.63 (m, 4H), 7.82 (m, 10H), 8.00 (d, J = 3.0 Hz, 1H), 8.92 (d, J = 3.0 Hz, 1H), 9.01 (d, J = 3.0 Hz, 1H), 10.44 (br s, 1H), 10.59 (br s, 1H). ^{13}C NMR (DMSO-d_6): δ 160.6, 156.2, 156.1, 141.9, 137.1, 136.7, 135.3, 130.8, 129.8, 129.65, 128.5, 124.8, 124.7, 124.5, 123.9, 122.6, 121.5, 120.8. MS (ESI): *m*/*z* 370.2 (M + 1), 353.1 (100%), 338.3, 311.1, 273.6. Anal. Calcd for $C_{21}H_{19}N_7 \cdot 3HCl \cdot 1.5H_2O$ (505.83): C, 49.86; H, 4.98; N, 19.38; Cl, 21.02. Found: C, 50.18; H, 4.96; N, 19.08; Cl, 20.96.

DNA Samples and Buffers. HBS-EP buffer (BIA Certified) from BIACORE contains 0.01 M HEPES (*N*-[2-hydroxyethyl]piperazine-*N*′-[2-ethanesulfonic acid]), 0.15 M NaCl, 3 mM EDTA, and 0.005% polysorbate 20 (v/v), pH 7.4. MES10 buffer was prepared with 0.01 M MES (2-(*N*-morpholino)ethanesulfonic acid), 0.001 M ethylenediaminetetraacetic acid (EDTA), and 0.1 M NaCl, and the pH was adjusted to 6.25 with NaOH solution. Polyd(A-T)$_2$, Polyd-(C-G)$_2$ and polydA·polydT were obtained from Pharmacia. 5′-Biotin (B) labeled hairpin duplexes for SPR[1] experiments (Midland Certified Reagent Co.-HPLC purified and desalted) are B-dCGAATTCGTCTCCGAATTCG (AATT hairpin), B-dCGAAATTTCTCTCGAAATTTCG (A3T3 hairpin), B-dCGATATCGTCTCCGATATCG (ATAT hairpin), B-dCATATATATCCCCATATATATG (AT hairpin), and B-dCGCGCGCGTTTTCGCGCGCG (CG hairpin), with the hairpin loop sequences underlined. The oligomer concentrations were determined optically using extinction coefficients per mole of strand at 260 nm determined by the nearest neighbor procedure: AATT hairpin (units of M (strand) $^{-1}$ cm^{-1}), E_{260} = 185 700; AT, E_{260} = 221 782; CG, E_{260} = 169 100; A3T3, E_{260} = 207 394; ATAT, E_{260} = 189 700.

Thermal Melting (T_m) Experiments. Experiments were conducted in MES10 as previously described. The concentration of the DNA was 5×10^{-5} M in base pairs, and the experiments were done using a Cary 300 spectrophotometer with the software supplied with the instrument.

Fluorescence Spectroscopy. Fluorescence spectra were obtained using a Cary eclipse spectrometer with software provided to control the instrument and collect the fluorescence data. Typically, the fluorescence intensity for the compound was measured at 25 °C in MES buffer, the samples were excited at 480 nm for ethidium and at 370 nm for DB950, and the fluorescence emission spectrum was collected. A solution of the compound was titrated with aliquots of DNA stock solution, and the samples were rescanned for the emission spectra.

Circular Dichroism. CD spectra were obtained on a Jasco J-810 spectrometer with software supplied by Jasco for instrument control, data acquisition, and manipulation. DNA solutions in MES10 buffer were scanned in 1 cm quartz cuvettes, aliquots of concentrated stock solutions of the compounds were titrated into DNA to give the desired ratio, and the complexes were rescanned.

Electric Linear Dichroism. Poly(dAT)$_2$ and poly(dGC)$_2$ were purchased from Sigma. Calf thymus DNA (Pharmacia) was deproteinized with sodium dodecyl sulfate (protein content <0.2%). All nucleic acids were extensively dialyzed against 1 mM sodium cacodylate buffered solution pH 7.0 prior to the ELD measurements performed with a computerized optical measurement system using the procedures previously outlined (*77*). All experiments were conducted with a 10 mm path length Kerr cell having 1.5 mm electrode separation. The samples were oriented under an electric field strength varying from 1 to 14 kV/cm. Unless specified, 10 μM of the tested drug was incubated with 200 μM of DNA. This electrooptical method senses only the orientation of the polymer-bound ligand: free ligand is isotropic and does not contribute to the signal (*78*).

Biosensor-Surface Plasmon Resonance (SPR). Binding and kinetics measurements were performed with BIAcore 2000 or 3000 systems and streptavidin coated sensor chips (CM-5 chips from BIAcore) as previously described (*79*, *80*). After covalent attachment of streptavidin by using a BIAcore supplied protocol, the chip surfaces were prepared for use

[1] Abbreviations: bp, base pair; SPR, surface plasmon resonance; TBE, Tris-borate-EDTA.

by conditioning with three to five consecutive 1 min injections of 1 M NaCl in 50 mM NaOH followed by extensive washing with buffer. 5′-Biotinylated DNA samples (25 nM) in HBS buffer were immobilized on the flow cell surface by noncovalent capture. Three flow cells were used to immobilize DNA oligomer samples, and the fourth cell was left blank as a control. Samples of the compounds were prepared in filtered and degassed MES10 buffer by serial dilution from stock solutions. Drug samples were injected at a flow rate of 20 μL/min using the KINJECT command. The same buffer solution was used to dissociate the compounds from DNA for surface regeneration. An array of different DB950 or ethidium concentrations, which yielded from little binding to saturation of the DNA sites, was used in each experiment, and the results were analyzed as described below. The injection of the compounds (association) was followed by injection of running buffer (compound dissociation). To reduce the probability of nonspecific binding to the chip surface, 50 μL/L of surfactant P20 was added to the MES buffers in the binding experiments. The amount of DNA immobilized was approximately 350−400 RU in each of the three flow cells. With the BIAcore SPR technique the change in resonance angle is monitored and reported in resonance units (RU). The increase in RU on compound injection is proportional to the amount of compound bound to the DNA.

To obtain the equilibrium binding constants, the data generated were fitted to different interaction models using Kaleidagraph for nonlinear least-squares optimization of the binding parameters using the equation

$$\mathrm{RU} = \mathrm{RU}_{\max}(K_1C_{\mathrm{free}} + 2K_1K_2C_{\mathrm{free}}{}^2)/(1 + K_1C_{\mathrm{free}} + K_1K_2C_{\mathrm{free}}{}^2) \quad (1)$$

where K_1 and K_2 are macroscopic equilibrium constants for two types of binding sites (for a single-site model $K_2 = 0$), RU is the SPR response at the steady-state level for each compound concentration, $\mathrm{RU}_{\max}$ is the maximum SPR response for binding one molecule per binding site, and C_{free} is the concentration of the compound in solution. $\mathrm{RU}_{\max}$ can be predicted using the equation

$$\mathrm{RU}_{\max} = (\mathrm{RU}_{\mathrm{DNA}}/\mathrm{MW}_{\mathrm{DNA}})\mathrm{MW}_{\mathrm{compound}}\,\mathrm{RII}$$

where $\mathrm{RU}_{\mathrm{DNA}}$ is the amount of DNA immobilized in response units (RU), MW is the molecular weight of compound and DNA, and RII is the refractive index increment ratio of compound to refractive index of DNA (*79*, *80*). $\mathrm{RU}_{\max}$ can also be used as a variable to be determined in the data fitting routines.

DNase I Footprinting. The plasmids were isolated from *E. coli* by a standard sodium dodecyl sulfate−sodium hydroxide lysis procedure and purified by banding in CsCl−ethidium bromide gradients. The 117 bp and 265 bp DNA fragments were prepared by 3′-[^{32}P]-end labeling of the *Eco*RI-*Pvu*II double digest of the pBS plasmid (Stratagene) using α-[^{32}P]-dATP (3000 Ci/mmol) and AMV reverse transcriptase. Similarly, the 176 bp fragment was prepared by 3′-[^{32}P]-end labeling of the *Eco*RI-*Pvu*II double digest of the pTUC plasmid. The labeled digestion products were separated on a 6% polyacrylamide gel under nondenaturing conditions in TBE buffer (89 mM Tris-borate pH 8.3, 1 mM EDTA). After autoradiography, the requisite band of DNA was excised, crushed, and soaked in water overnight at 37 °C. This suspension was filtered, and the DNA was precipitated with ethanol. DNase I footprinting experiments were performed essentially as previously described (*81*). Briefly, samples (3 μL) of the labeled DNA fragments were incubated with 5 μL of the buffered solution containing the ligand at appropriate concentration. After 30 min incubation at 37 °C to ensure equilibration of the binding reaction, the digestion was initiated by the addition of 2 μL of a DNase I solution, whose concentration was adjusted to yield a final enzyme concentration of about 0.01 unit/mL in the reaction mixture. After 3 min, the reaction was stopped by freeze-drying. Samples were lyophilized and resuspended in 5 μL of an 80% formamide solution containing tracking dyes. The DNA samples were then heated at 90 °C for 4 min and chilled in ice for 4 min prior to electrophoresis on a 8% polyacrylamide gel under denaturing conditions (8 M urea). A Molecular Dynamics 425E PhosphorImager was used to collect data from the storage screens exposed to dried gels overnight at room temperature. Baseline-corrected scans were analyzed by integrating all the densities between two selected boundaries using ImageQuant version 3.3 software. Each resolved band was assigned to a particular bond within the DNA fragments by comparison of its position relative to sequencing standards generated by treatment of the DNA with dimethyl sulfate followed by piperidine-induced cleavage at the modified guanine bases in DNA (G-track).

Scheme 1. Synthesis of DB950[a]

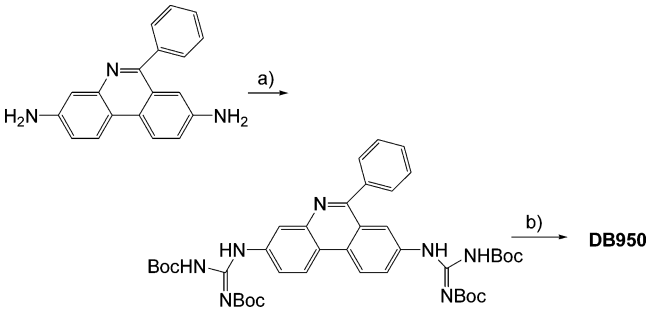

[a] Reagents and conditions: (a) (MeS)(NHBoc)C═NBoc, $HgCl_2$, TEA, DMF, room temperature; (b) HCl, CH_2Cl_2, EtOH, room temperature.

RESULTS

Chemistry. The synthesis of 3,8-bis(guanidino)-6-phenylphenanthridine (**3**) is outlined in Scheme 1 and employs methodology that we have used previously for the preparation of aryl guanidines (*82*, *83*). 3,8-Diamino-6-phenylphenanthridine (**1**) was converted into the tetra-Boc analogue **2** using mercury(II) chloride facilitated guanidylation with bis(*tert*-butoxycarbonyl)-2-methyl-2-thiopseudourea. Deprotection of **2** at room temperature with HCl in dichloromethane at room temperature gave the trihydrochloride salt of **3**.

Binding Affinity and Compound Structure: ΔT_m Measurements. T_m increases relative to uncomplexed DNA (ΔT_m) for compound complexes at specific DNA sequences provide an excellent method for ranking compound binding affinities at different sequences (*84*). The T_m increases caused by the compounds in Figure 1 have been determined for their

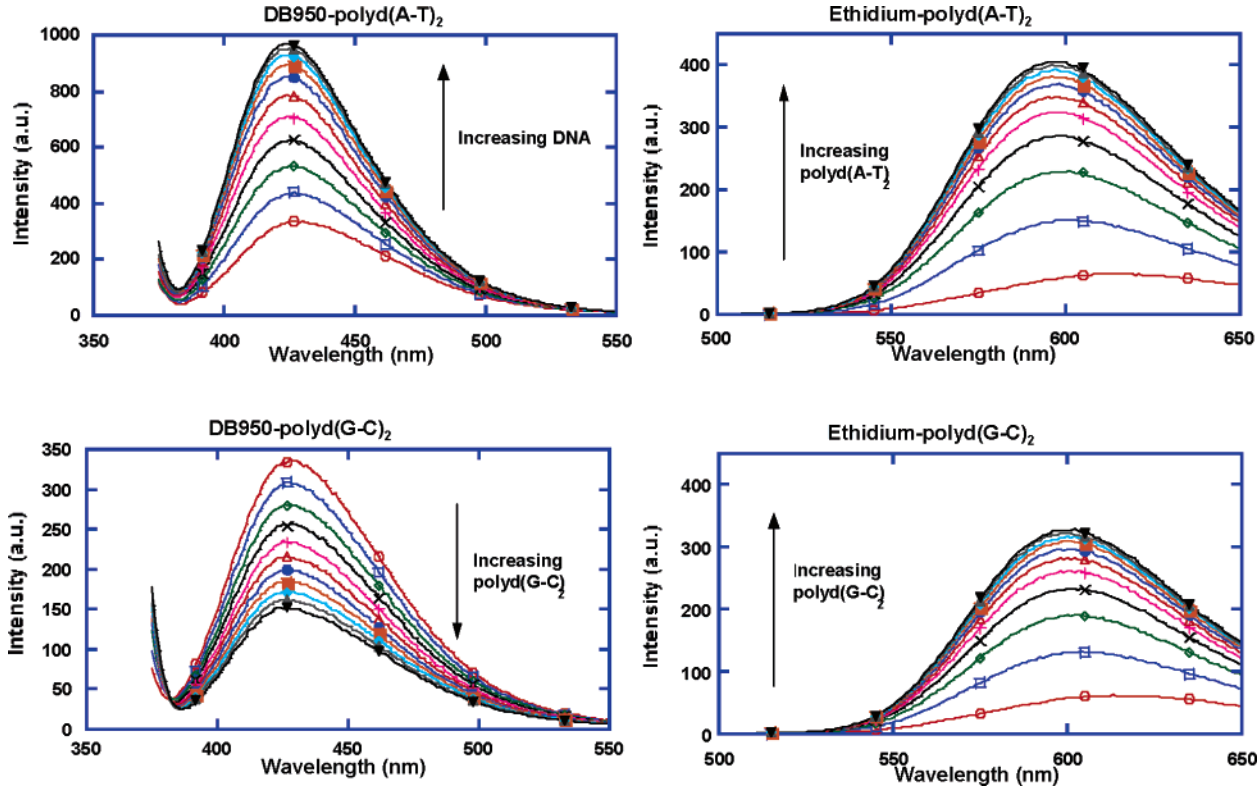

FIGURE 2: Fluorescence emission spectral titrations of DB950 and ethidium with polyd(A-T)$_2$ and polyd(G-C)$_2$. Titrations were conducted in MES10 buffer in a 1 cm cell at 25 °C with the compounds at 1×10^{-6} M. The excitation wavelength for DB950 was 370 nm and for ethidium was 480 nm; the excitation slit was at 5 nm and the emission slit at 20 nm.

complexes with an AT polymer as a reference point. With this polymer ethidium has a ΔT_m value of 5.7 °C, while DB950 has a higher value of 16.0 °C. With AATT oligomer ethidium has a ΔT_m value of 1.7 °C, while DB950 again has a value of 6.4 °C. In summary, these results agree with those from DNaseI footprinting (see below) and qualitatively show that it is possible to significantly enhance the AT binding affinity of ethidium through the change of the amines to guanidinium groups.

Absorption and Fluorescence Emission Spectroscopy. Absorption spectra for DB950 and ethidium are shown in Figure S1 (Supporting Information), and fluorescence emission spectra are in Figure 2 for titrations with polyd(A-T)$_2$. Both the absorption and the emission spectra are strongly perturbed when the two compounds form complexes with DNA. Ethidium has similar induced spectral changes on complex formation with polyd(A-T)$_2$ and polyd(G-C)$_2$, while changes induced by binding of DB950 to the two polymers are quite different (Figure 2). Ethidium also has similar changes in fluorescence intensity on titration with polyd(A-T)$_2$ and polyd(C-G)$_2$. The emission intensity of DB950 on the other hand increased on addition of polyd(A-T)$_2$ and decreased on addition of polyd(G-C)$_2$. The AT and GC spectral changes occur at similar concentrations for ethidium, while much higher concentrations of DB950 are required in the GC titrations.

Binding Mode: Circular Dichroism (CD) Spectroscopy. Binding of DB950 to polyd(A-T)$_2$ was characterized by CD spectroscopy in the wavelength range between 220 and 400 nm and for ethidium from 200 to 500 nm (Figures 3 and S3). CD spectra monitor the asymmetric environment of the compounds when bound to DNA and therefore can be used to obtain information on the binding mode. The free

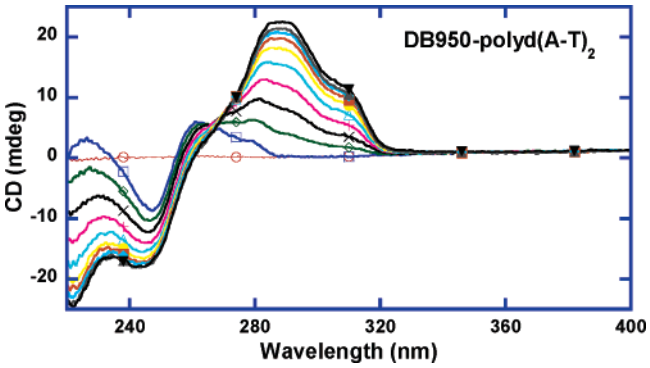

FIGURE 3: CD spectral titrations of DB950 with polyd(A-T)$_2$. Strong induced signals are observed with increasing ratio of compound to DNA. The ratios of compound to DNA base pairs are 0, 0.05, 0.10, 0.15, 0.20, 0.25, 0.30, 0.35, 0.40, and 0.50. The experiments were conducted at 25 °C in MES 10, and the DNA concentration was 2×10^{-5} M (in base pairs).

compounds do not exhibit CD signals; however, upon addition of the compounds to DNA, substantial positive CD signals arise between 270 and 320 nm. This large induced CD can represent a characteristic pattern for a minor groove-binding mode of aromatic cations (*85*, *86*). Ethidium has positive induced CD signals in the wavelength range below 350 nm with polyd(A-T)$_2$ but has no significant induced CD bands in its long-wavelength absorption region above 400 nm (Figure S2). Isoelliptic points are observed in the titration of DB950 with DNA at 270 nm with significantly larger positive induced CD signals at 290 nm. Isoelliptic points are observed for the ethidium−DNA complex at 230 and 270 nm with smaller induced CD signals. In conclusion, induced CD spectra on binding of DB950 to polyd(A-T)$_2$ are consistent with a minor groove binding mode for this

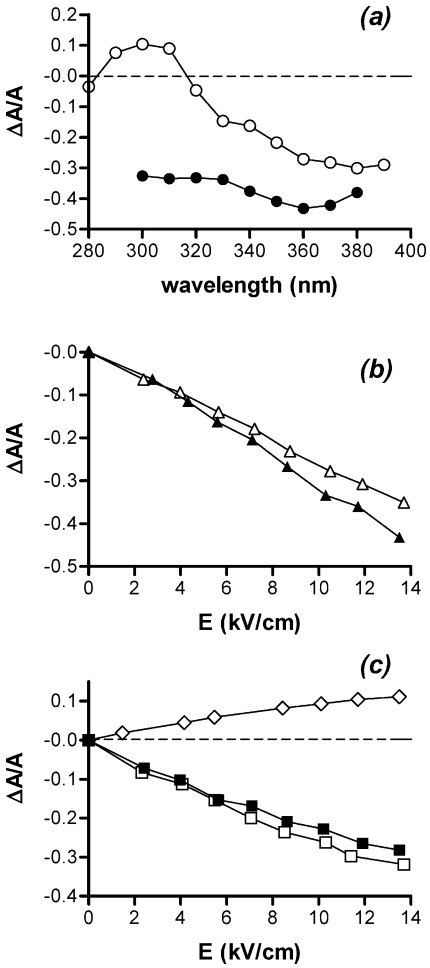

FIGURE 4: (a) Electric linear dichroism spectra of DB950 bound to the alternating polymers (○) poly(dAT)$_2$ and (●) poly(dGC)$_2$. ELD spectra were recorded at 13.5 kV/cm and at a P/D ratio of 20 (200 μM DNA, 10 μM drug). (b) Dependence of the reduced dichroism $\Delta A/A$ on the electric field strength for (△) poly(dGC)$_2$ and (▲) its complex with DB950. (c) Dependence of the reduced dichroism $\Delta A/A$ on the electric field strength for (◇) poly(dAT)$_2$ and its complex with DB950 measured (□) at 300 nm or (■) 370 nm. Conditions: P/D = 20 (200 μM DNA, 10 μM drug), 300, and 370 nm for drug−DNA complexes and 260 nm for the DNA alone. All measurements were performed at room temperature (20 °C) in 1 mM sodium cacodylate buffer, pH 7.0.

compound, in contrast to the well-known intercalation mode for ethidium.

Electric Linear Dichroism (ELD) is another spectroscopic method using polarized light that is useful to study the mechanism of binding of small molecules to DNA. We employed this method to compare the binding of DB950 with that of the parent compounds. Ethidium bromide gave identical ELD signals upon binding to polyd(A-T)$_2$ and polyd(G-C)$_2$, with negative amplitudes characteristic of an intercalating agent (Figure S3). In contrast, as expected, DB75 gave positive signals with polyd(A-T)$_2$ and negative signals with polyd(G-C)$_2$ (Figure S3). We have previously shown that the diphenylfurans, including furamidine, exhibit distinct modes of binding to AT and GC sequences (*87*). The behavior of DB950 is similar to that of DB75, with a negative ELD values recorded in the presence of polyd(G-C)$_2$ and positive ELD values in the presence of polyd(A-T)$_2$ at 300 nm (Figure 4). With this AT polymer, the ELD is positive in the 290−310 nm region and negative in the 320−390 region of the absorption spectra for the DB950-DNA complexes (Figure 4). The occurrence of positive ELD signals in the 300 nm region in the presence of polyd(A-T)$_2$ excludes intercalation and confirms the conclusion of the CD measurements that the drug forms minor groove complexes at AT sequences. The CD and ELD data together establish that the incorporation of the guanidinium groups on the ethidium skeleton are sufficient to allow minor groove binding to AT sites. ELD measurements have been also performed with a composite DNA from calf thymus (42% GC), and in this case negative ELD signals were recorded in the presence of DB950 (Figure S4) but the two distinct binding modes at AT and GC sites cannot be distinguished in this case. The intense negative signals due to the intercalated molecules certainly mask the signals arising from the molecules bound in the groove.

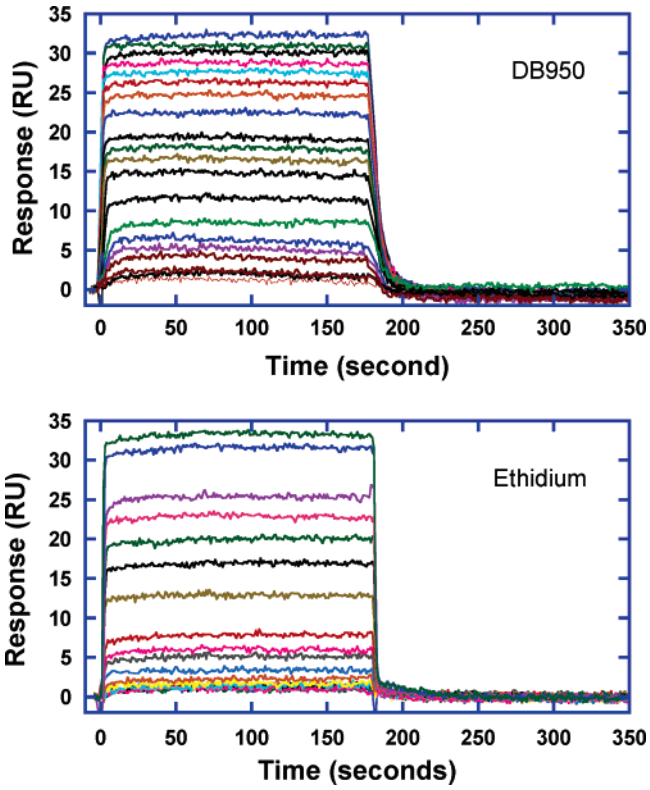

FIGURE 5: SPR sensorgrams for the interaction of DB950 and ethidium with the A3T3 hairpin duplex DNA. The concentrations are from 1×10^{-8} M (lower curves) to 1×10^{-5} M (highest curves). The experiments were conducted at 25 °C in MES 10 with a flow rate of 20 μL/min.

Binding Affinity, Cooperativity, and Stoichiometry: Biosensor-SPR Experiments. Biosensor-SPR methods are excellent for determination of stoichiometry, cooperativity, and affinity in DNA oligomer−small molecule complexes. Radiolabeling is not required, and each bound molecule yields the same signal increase so that stoichiometry can be obtained independently of data fitting (see Materials and Methods). Sensorgrams (RU versus time for a DNA flow cell−a blank) for binding of these compounds to the immobilized A3T3 hairpin duplex sequence (Materials and Methods) are compared in Figure 5. With both compounds the kinetics of association with and dissociation from DNA are quite rapid, and a steady-state plateau is reached in the sensorgrams in a short time under all experimental concentrations (Figure 5). The binding constants were obtained from plotting the

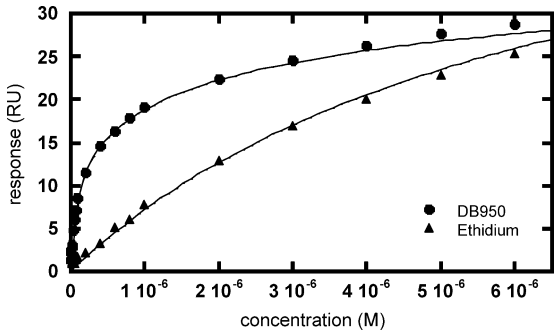

FIGURE 6: RU values for binding of DB950 and ethidium to A3T3 from the steady-state regions of the sensorgrams in Figure 5 are plotted versus the free compound concentration (controlled by the flow solution). The points in the figure are experimental, and the lines are the best fit values to the two-site model described in Materials and Methods. The *K* values are in Table 1 and for ethidium K1 and K2 are identical within experimental error.

Table 1: SPR Binding Constants (K, M^{-1}) for the Compounds to Different DNA Sequences[a]

	DB950		ethidium
sequence	K_1	K_2	K
A_3T_3	8.2×10^6	2.3×10^5	1.5×10^5
A_2T_2	4.7×10^6	9.4×10^4	1.4×10^5
ATAT	9.6×10^6	7.1×10^4	4.2×10^5
$(AT)_4$	3.5×10^6	2.5×10^6	2.1×10^5
$(CG)_4$	3.5×10^5		1.6×10^5

[a] Experiments were conducted in MES10 buffer at 25 °C. The *K* values are best-fit values to a two-site binding model (Materials and Methods). With ethidium the two *K* values are very similar, and the average is shown. DNA used: B-dCGAATTCGTCTCCGAATTCG (AATT hairpin), B-dCGAAATTTCTCTCGAAATTTCG (A3T3 hairpin), B-dCGATATCGTCTCCGATATCG (ATAT hairpin), B-dCATATATATCCCCATATATATG (AT hairpin), and B-dCGCG-CGCGTTTTCGCGCGCG (CG hairpin).

average response at steady state versus the free compounds concentrations and the data fitted using eq 1. Direct plots for DB950 and ethidium binding to the A3T3 are shown in Figure 6 and plots of similar shape were obtained for ethidium. The curve for DB950 was best fit with an equation that has two types of binding sites for the compound on the DNA (Methods) on the other hand the ethidium curve was fit with one class binding sites with a stoichiometry of 2−3 (eq 1). In the case of DB950 there was one strong binding site and a second site with significantly weaker binding. With DB950 binding to the A3T3 DNA, for example, the strong site has a *K* value of 1.0×10^7 M^{-1} with a secondary binding *K* of 2×10^5 M^{-1}. The *K* value for DB950 binding to the CG oligomer sequence, $K = 3.8 \times 10^5$ M^{-1}, is approximately 30 times lower than that for binding to the A3T3 sequence. The binding constants to the other AT sequences are compared in Table 1. The stronger binding to AT sequences agrees with the footprinting and T_m results. DB950 binds better to the AAATTT than to the shorter AATT sequence, suggesting that it may fit better in sites that are somewhat longer than four base pairs. Ethidium binds similarly to the two sequences, as would be expected for an intercalation-binding mode.

Sequence Selectivity. The capacity of DB950 to bind preferentially to defined sequences in DNA was investigated by the DNase I fooprinting methodology. This gel-based technique has been instrumental to probe sequence recognition by a variety of small molecules, both intercalators and groove binders (*88*). Three DNA restriction fragments of 117, 176, and 265 bp were purified and 3′-end radiolabeled with ^{32}P. DNA and drug−DNA complexes were then partially digested under controlled conditions (single hit kinetics) (*81*) with DNase I, and the resulting digestion products were resolved on polyacrylamide sequencing gels. DNase I cuts DNA at every bp position within the sequences, but the intensity of cleavage varies from one phosphodiester bond to another, depending on the sequence context. However, the preference is sufficiently low to enable cleavage at almost all internucleotide bonds, thus providing a nonuniform ladder of bands in the drug-free control lanes. In the presence of DB950, it can be seen immediately, simply from looking at the gels (Figure 7), that the cleavage becomes even less uniform, and marked footprints can be seen in some places, such as around nucleotide positions 56, 75, and 100 on the 176 bp fragment for example. The footprinting patterns obtained with DB950 are very distinct from those produced by ethidium bromide. The sites of DNase I cleavage protected by ethidium do not coincide with footprints seen with DB950 and, conversely, the sites where the cleavage by the enzyme is markedly enhanced by ethidium generally correspond to preferential binding sites (footprints) for DB950. In fact, the footprinting patterns seen with DB950 are comparable to those produced by DB75. These two drugs give rise to strong footprints around positions 53 and 75 on the 265 bp DNA fragment, for examples. With the three DNA fragments, the profiles for DB75 and DB950 are very similar and footprints develop in the same concentration range (Figure 7).

Gels were analyzed by densitometry, from which differential cleavage plots were drawn to estimate the location and relative strength of binding at particular DNA sequences (Figure 8). The dips in these plots (negative values) indicate sites of protection from DNase I cleavage, whereas peaks (positive values) indicate regions of drug-induced enhancement of nuclease cleavage. The plots resulting from the DNase I treatment of ethidium−DNA complexes are considerably different from those obtained with DB950. Ethidium can protect from DNase I cleavage a variety of sequences containing mixed AT and GC base pairs. The most pronounced footprints with ethidium occur at two sites encompassing the sequence 5′-CTCACTA, found around nucleotide positions 65 and 68 on the 176 bp and 265 bp fragments, respectively. However, the ethidium profiles are essentially characterized by sites of enhanced cleavage by DNase I. Several sequences containing short runs of contiguous $(A)_n$-$(T)_n$ become much more sensitive to DNase I in the presence of ethidium compared to the control drug-free lanes. For example, the $(A)_4$-$(T)_4$ tracts at positions 54 (265 bp), 99 (176 bp), and 64 (117 bp) are strongly cleaved by the enzyme in the presence of ethidium. In sharp contrast, the same sequences are protected from the enzyme cleavage in the presence of DB950. In fact, the cleavage plots for ethidium and DB950 more or less look like mirror images: a site of cleavage enhancement by ethidium often coincides with a footprint for DB950 and vice versa. All sequences protected from cleavage by DB950 are composed of at least 4 A-T bp (e.g. 5′-AATT, 5′-ATTA, 5′-AATA, 5′-AAAA, 5′-TTAA). There is absolutely no doubt that, unlike ethidium, DB950 exhibits a strict preference for AT sites. The cleavage plots for DB950 are very similar to those obtained with DB75

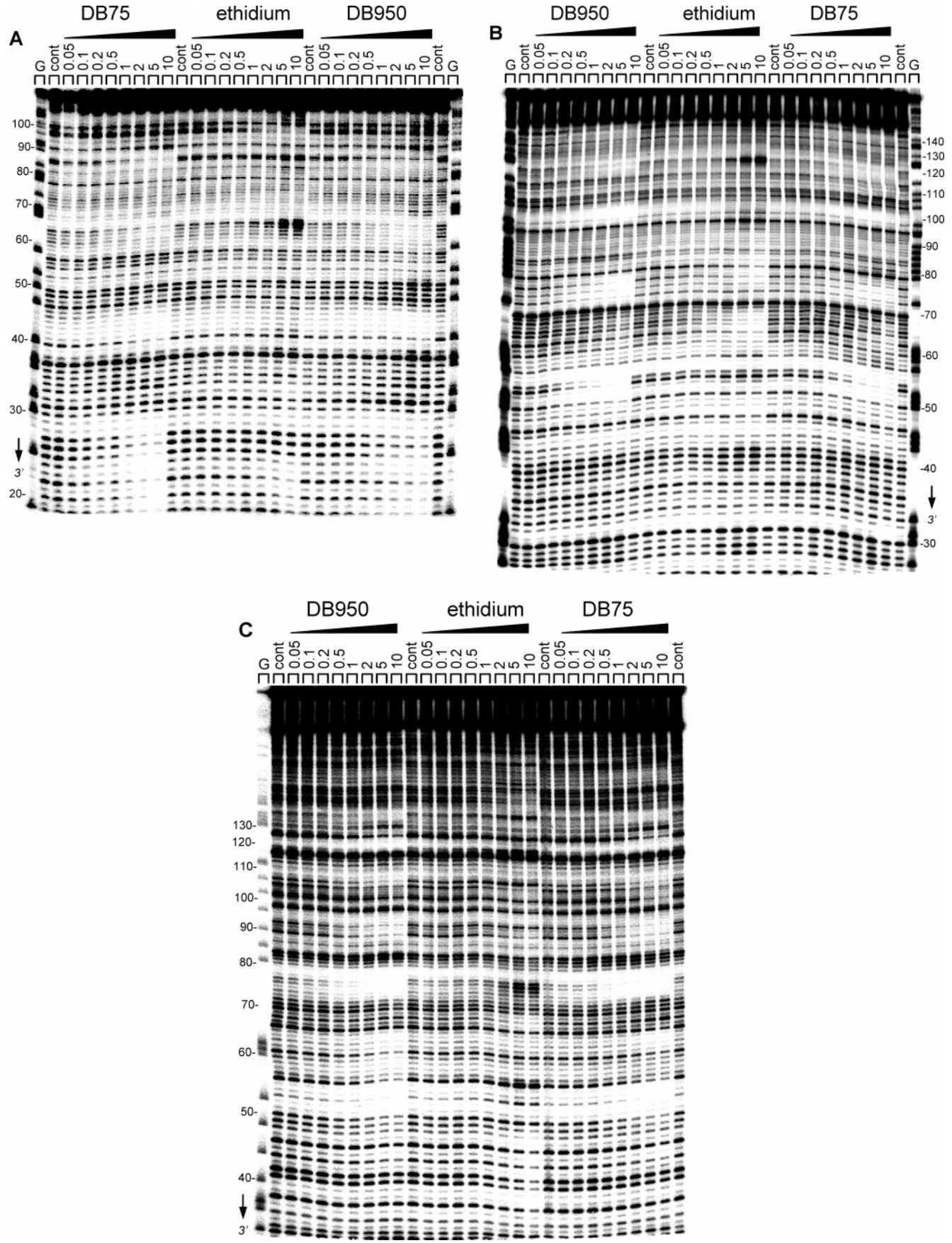

FIGURE 7: Sequence selective binding of DB75, ethidium, and DB950. The gels show DNase I footprinting with three 3′-end labeled DNA restriction fragments of (A) 117, (B) 176, and (C) 265 base pairs. The products of nuclease digestion were resolved on an 8% polyacrylamide gel containing 7 M urea. Control tracks (marked Ct) contained no drug. Guanine-specific sequence markers obtained by treatment of the DNA with dimethyl sulfate followed by piperidine were run in the lanes marked G. Numbers on the side of the gels refer to the standard numbering scheme for the nucleotide sequence of the DNA fragment.

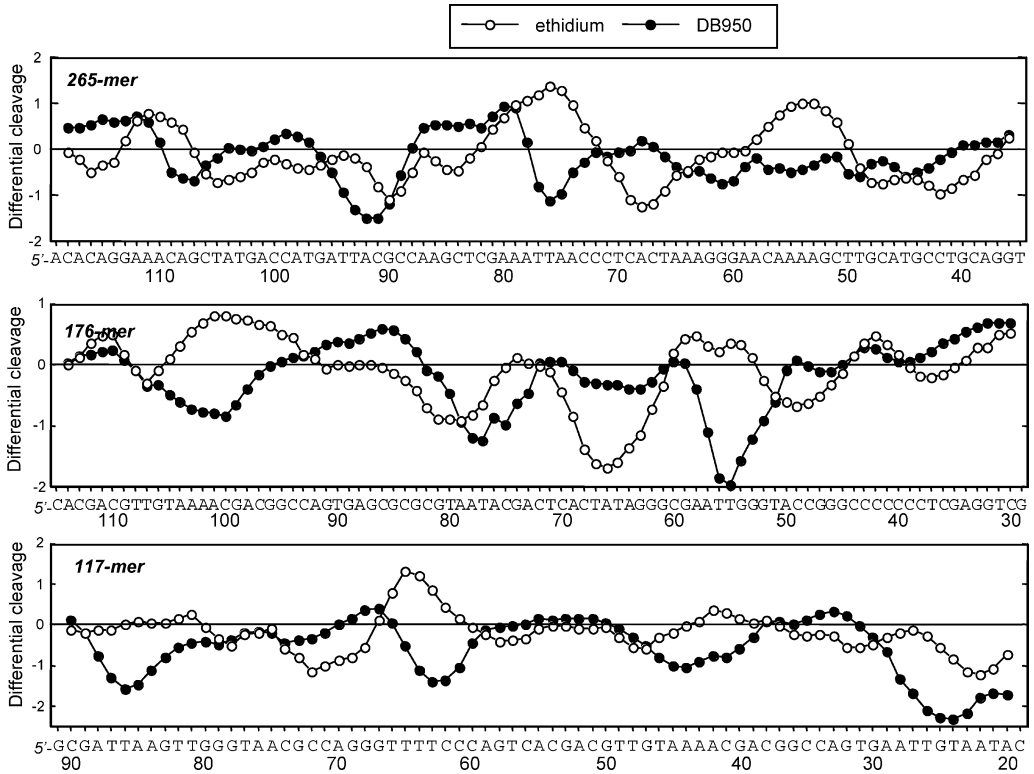

FIGURE 8: Differential cleavage plots comparing the susceptibilities of the different DNA fragments to DNase I cutting in the presence of ethidium and DB950 at the indicated concentrations. Negative values correspond to a ligand-protected site, and positive values represent enhanced cleavage. Vertical scales are in units of $\ln(f_a) - \ln(f_c)$, where f_a is the fractional cleavage at any bond in the presence of the drug and f_c is the fractional cleavage of the same bond in the control, given closely similar extents of overall digestion. Each line drawn represents a three-bond running average of individual data points, calculated by averaging the value of $\ln(f_a) - \ln(f_c)$ at any bond with those of its two nearest neighbors. Only the region of the restriction fragments analyzed by densitometry is shown.

(Figure S5), and this is consistent with their identical DNA minor groove binding modes.

DISCUSSION

The synthesis of DB950 exploits a long-established experience for the preparation of aryl guanidines (*82*, *83*). At first sight, this compound was thought to be "just an ethidium analog", but the study of its DNA binding properties revealed considerable differences between the two molecules. It became rapidly evident that DB950 exhibited DNA recognition properties significantly distinct from those of ethidium but similar to those of DNA minor groove binders. Therefore, we incorporated in our study the diamidino compound DB75 (furamidine), which has been extensively characterized as a DNA minor groove binder. High-resolution structural data are available for furamidine-d(CGCGAATTCGCG)$_2$ complexes and related compounds (*89*−*92*) and their sequence recognition, kinetics of binding, and sequence-dependent affinity have been also scrutinized (*93*). DB75 binds very tightly to the minor groove at $(A/T)_4$ sites, but it can also interact with GC sites via an intercalative binding mode. Unfused aromatic cations, including diphenylfurans and other extended benzimidazole-containing dications (e.g. DAPI, Hoechst 33258), exhibit dual binding properties (*87*). Despite its distinct structure, DB950 shares this dual property. The fluorescence titrations indicated that DB950 interacts differently with the AT and GC polymers. While the fluorescence of ethidium was similarly affected by addition of polyd(A-T)$_2$ and polyd(C-G)$_2$, the emission intensity of DB950 increased only with polyd(A-T)$_2$ and decreased with polyd(G-C)$_2$. However, the binding mode cannot be unambiguously defined from fluorescence measurements (*94*). We therefore used CD and ELD spectroscopy to establish that DB950 forms minor groove complexes at AT sites. This binding process is with no doubt at the origin of the strong footprints detected at AT sequences in the presence of DB950. The bis-guanidinium compound also interacts with GC sites, via an intercalation process as revealed by the ELD measurements, but the SPR analysis indicates that binding to the GC oligomer is 30 times weaker than binding to the A3T3 oligomer. This is why the footprinting experiments only reveal the interaction at AT sites.

The change of the amine groups of ethidium for guanidinium groups significantly reinforces the DNA binding strength and has a considerable effect on sequence recognition. DB950 gives much higher ΔT_m values with both the poly(dAT)$_2$ polymer and AATT oligomer. The gain of affinity for AT sites, quantified by SPR using A_nT_n hairpin duplexes, is considerable. DB950 binds 55 and 12 times more tightly to A3T3 and A2T2 than ethidium, and the binding constants for DB950 approach those previously reported with furamidine (*93*). The fact that furamidine and DB950 bind equally tightly to AT sequences and exhibit a sharp preference for identical sites strongly suggests that their selectivity arises principally from the terminal cationic groups. The amidinium or guanidinium groups serve to anchor the drug in the minor groove. These two types of cationic groups provide similar binding strengths for DNA. The DNA interaction of 2,5-diarylfurans bearing amidine or guanidine terminal groups has been studied, and indeed, little difference

in affinity was observed (*82*, *95*). The sharp selectivity of DB950 for AT sites and its capacity to fit into the DNA minor groove reflect the major contribution of the guanidium groups. Amidinium or guanidinium groups contribute importantly to the high affinity and AT selectivity of minor groove binders (*96*−*98*).

Ethidium analogues structurally related to DB950 have been recently reported. Tor and co-workers have shown that the affinity and selectivity of ethidium for a given RNA target, the HIV-1 Rev Response Element (RRE), can be profoundly modulated by converting the two amine groups of ethidium with urea, pyrrole, or guanidinium groups (*71*). One of the compounds mentioned in this study was a bis-guanidinium−ethidium derivative almost identical with DB950, which was found to bind to calf thymus DNA 6 times more tightly than ethidium. This is in agreement with our study, which goes further in terms of characterization of the DNA binding mechanism, revealing a sequence-dependent binding interaction. Together, these two studies establish that the chemical modulation of the ethidium exocyclic amines is a profitable option to tune the nucleic acid recognition properties of phenylphenanthridiniums.

There have been examples in the past of AT-selective DNA minor groove binders, such as DAPI and pibenzimol (Hoechst 33258), that were later shown to intercalate at GC (*13*−*15*). Here we show that the converse situation is also possible: a well established intercalating agent can be modified to adapt to the minor groove of DNA. DNA is a versatile object which can be targeted in different ways with various tools. After half a century of work of DNA binding small molecules, we are approaching a situation where almost any cleft (lock) in the double helix (and in more complex multistranded structures as well) can be recognized by a ligand (key). By looking through the keyholes, we will hopefully better understand how to manipulate the genetic code.

SUPPORTING INFORMATION AVAILABLE

Five figures showing the absorption spectra and circular dichroism and electric linear dichroism data for the compounds. This material is available free of charge via the Internet at http://pubs.acs.org.

REFERENCES

1. Demeunynck, M., Bailly, C., and Wilson, W. D. (2003) *DNA and RNA Binders*, Wiley-VCH, Weinheim, Germany.
2. Waring, M. J. (1981) DNA modification and cancer. *Annu. Rev. Biochem. 50*, 159−192.
3. Neidle, S. (2001) DNA minor-groove recognition by small molecules. *Nat. Prod. Rep. 18*, 291−309.
4. Dervan, P. B. (2001) Molecular recognition of DNA by small molecules. *Bioorg. Med. Chem. 9*, 2215−2235.
5. Hurley, L. H. (2002) DNA and its associated processes as targets for cancer therapy. *Nat. Rev. Cancer 2*, 188−200.
6. Lerman, L. S. (1961) Structural considerations in the interaction of DNA and acridines. *J. Mol. Biol. 3*, 18−30.
7. Waring, M. J. (1968) Drugs which affect the structure and function of DNA. *Nature 219*, 1320−1325.
8. Zimmer, C., and Wähnert, U. (1986) Nonintercalating DNA-binding ligands: specificity of the interaction and their use as tools in biophysical, biochemical and biological investigations of the genetic material. *Prog. Biophys. Mol. Biol. 47*, 31−112.
9. Neidle, S., and Abraham, Z. (1984) Structural and sequence-dependent aspects of drug intercalation into nucleic acids. *CRC Crit. Rev. Biochem. 17*, 73−121.
10. Besterman, J. M., Elwell, L. P., Blanchard, S. G., and Cory, M. (1987) Amiloride intercalates into DNA and inhibits DNA topoisomerase II. *J. Biol. Chem. 262*, 13352−13358.
11. Bailly, C., Cuthbert, A. W., Gentle, D., Knowles, M. R., and Waring, M. J. (1993) Sequence-selective binding of amiloride to DNA. *Biochemistry 32*, 2514−2524.
12. Wakelin, L. P. G., Adams, A., Hunter, C., and Waring, M. J. (1981) Interaction of crystal violet with nucleic acids. *Biochemistry 20*, 5779−5787.
13. Wilson, W. D., Tanious, F. A., Barton, H. J., Strekowski, L., and Boykin, D. W. (1989) Binding of 4′-6-diamidino-2-phenylindole (DAPI) to GC and mixed sequences in DNA: intercalation of a classical groove-binding molecules. *J. Am. Chem. Soc. 111*, 5008−5010.
14. Wilson, W. D., Tanious, F. A., Barton, H. J., Jones, R. L., Fox, K. R., Wydra, R. L., and Strekowski, L. (1990) DNA sequence dependent binding modes of 4′-6-diamidino-2-phenylindole (DAPI). *Biochemistry 29*, 8452−8461.
15. Bailly, C., Hénichart, J. P., Colson, P., and Houssier, C. (1992) Drug−DNA sequence-dependent interactions analysed by electric linear dichroism. *J. Mol. Recognit. 5*, 155−171.
16. Boykin, D. W., Kumar, A., Bender, B. K., Hall, J. E., and Tidwell, R. R. (1996) Anti-Pneumocystis activity of bis-amidoximes and bis-O-alkylamidoximes prodrugs. *Bioorg. Med. Chem. Lett. 6*, 3017−3020.
17. Tidwell, R. R., and Boykin, D. W. (2003) Dicationic DNA minor groove binders as antimicrobial agents. In *DNA and RNA Binders* (Demeunynck, M., Bailly, C., Wilson, W. D., Eds.), pp 414−460, Wiley-VCH, Weinheim, Germany.
18. Neidle, S., Kelland, L. R., Trent, J. O., Simpson, I. J., Boykin, D. W., Kumar, A., and Wilson, W. D. (1997) Cytotoxicity of bis-(phenylamidinium)furan alkyl derivatives in human tumour cell lines: Relation to DNA minor groove binding. *Bioorg. Med. Chem. 7*, 1403−1408.
19. Fuller, W., and Waring, M. J. (1964) Molecular model for the interaction of ethidium bromide with DNA. *Ber. Bunsen-Ges. Phys. Chem. 68*, 805−808.
20. Waring, M. J. (1965) Complex formation between ethidium bromide and nucleic acids. *J. Mol. Biol. 13*, 269−282.
21. Crawford, L. V., and Waring, M. J. (1967) Supercoiling of polyoma virus DNA measured by its interaction with ethidium bromide. *J. Mol. Biol. 25*, 23−30.
22. Waring, M. J. (1970) Variation of the supercoils in closed circular DNA by binding of antibiotics and drugs. Evidence for molecular models involving intercalation. *J. Mol. Biol. 54*, 247−279.
23. Tsai, C. C., Jain, S. C., and Sobell, H. M. (1975) X-ray crystallographic visualization of drug-nucleic acid intercalative binding: structure of an ethidium-dinucleoside monophosphate crystalline complex, ethidium: 5-iodouridylyl (3′-5′) adenosine. *Proc. Natl. Acad. Sci. U.S.A. 72*, 628−632.
24. Liebman, M., Rubin, J., and Sundaralingam, M. (1977) Nonintercalative binding of ethidium bromide to nucleic acids: Crystal structure of an ethidium-tRNA molecular complex. *Proc. Natl. Acad. Sci. U.S.A. 74*, 4821−4825.
25. Le Pecq, J. B., and Paoletti, C. (1967) A fluororescent complex between ethidium bromide and nucleic acids. *J. Mol. Biol. 27*, 87−106.
26. Morgan, A. R., Lee, J. S., Pulleyblank, D. E., Murray, N. L., and Evans, D. H. (1979) Review: ethidium fluorescence assays. Part 1. Physicochemical studies. *Nucleic Acids Res. 7*, 547−569.
27. Baguley, B. C., and Falkenhaug, E.-M. (1978) The interaction of ethidium with synthetic double-stranded polynucleotides at low ionic strength. *Nucleic Acids Res. 5*, 161−171.
28. Krugh, T. R., and Reinhardt, C. G. (1975) Evidence for sequence preferences in the intercalative binding of ethidium to dinucleotide monophosphates. *J. Mol. Biol. 97*, 133−162.
29. Wilson, W. D., and Jones, R. L. (1982) Interaction of actinomycin D, ethidium, quinacrine, daunorubicin, and tetralysine with DNA: ^{31}P NMR chemical shift and relaxation investigation. *Nucleic Acids Res. 10*, 1399−1410.
30. Chandrasekaran, S., Krishnamoorthy, C. R., Jones, R. L., Smith, J. C., and Wilson, W. D. (1984) Stopped-flow kinetic, ^{1}H, and ^{31}P NMR analysis of the intercalation of ethidium with poly d(G−C)xd(G−C). *Biochem. Biophys. Res. Commun. 122*, 804−809.
31. Chandrasekaran, S., Jones, R. L., and Wilson, W. D. (1985) Imino ^{1}H- and ^{31}P NMR analysis of the interaction of propidium and ethidium with DNA. *Biopolymers 24*, 1963−1979.
32. Wilson, W. D., Krishnamoorthy, C. R., Wang, Y. H., and Smith, J. C. (1985) Mechanism of intercalation: ion effects on the

equilibrium and kinetic constants for the interaction of propidium and ethidium with DNA. *Biopolymers 24*, 1941−1961.
33. Bresloff, J. L., and Crothers, D. M. (1981) Equilibrium studies of ethidium-polynucleotide interactions. *Biochemistry 20*, 3547−3553.
34. Hernandez, L. I., Zhong, M., Courtney, S. H., Marky, L. A., and Kallenbach, N. R. (1994) Equilibrium analysis of ethidium binding to DNA containing base mismatches and branches. *Biochemistry 33*, 13140−13146.
35. Ren, J., and Chaires, J. B. (2001) Rapid screening of structurally selective ligand binding to nucleic acids. *Methods Enzymol. 340*, 99−108.
36. Meyer-Almes, F. J., and Porschke, D. (1993) Mechanism of intercalation into the DANN double helix by ethidium. *Biochemistry 32*, 4246−4253.
37. Marky, L. A., and McGregor, R. B. J. (1990) Hydration of dA.dT polymers: role of water in the thermodynamics of ethidium and propidium intercalation. *Biochemistry 29*, 4805−4811.
38. Hopkins, H. P., Jr., and Wilson, W. D. (1987) Enthalpy and entropy changes for the intercalation of small molecules to DNA. II. Ethidium and propidium fluoride. *Biopolymers 26*, 1347−1355.
39. Hopkins, H. P., Jr., Fumero, J., and Wilson, W. D. (1990) Temperature dependence of enthalpy changes for ethidium and propidium binding to DNA: effect of alkylamine chains. *Biopolymers 29*, 449−459.
40. Ren, J., Jenkins, T. C., and Chaires, J. B. (2000) Energetics of DNA intercalation reactions. *Biochemistry 39*, 8439−8447.
41. Vergani, L., Gavazzo, P., Mascetti, G., and Nicolini, C. (1994) Ethidium bromide intercalation and chromatin structure: A spectropolarimetric analysis. *Biochemistry 33*, 6578−6585.
42. Houssier, C., Hardy, B., and Fredericq, E. (1974) Interaction of ethidium bromide with DNA. Optical and electrooptical study. *Biopolymers 13*, 1141−1160.
43. Gatti, C., Houssier, C., and Fredericq, E. (1975) Binding of ethidium bromide to ribosomal RNA. Absorption, fluorescence, circular and electric dichroism study. *Biochim. Biophys. Acta 407*, 308−319.
44. Yoshida, H., Swenberg, C. E., and Geacintov, N. E. (1987) Kinetic flow dichroism study of conformational changes in supercoiled DNA induced by ethidium bromide and noncovalent and covalent binding of benzo[*a*]pyrene diol epoxide. *Biochemistry 26*, 1351−1358.
45. Swenberg, C. E., Carberry, S. E., and Geacintov, N. E. (1990) Linear dichroism characteristics of ethidium- and proflavine-supercoiled DNA complexes. *Biopolymers 29*, 1735−1744.
46. Yao, S., and Wilson, W. D. (1992) A molecular mechanics investigation of RNA complexes. I. Ethidium intercalation in an HIV-1 TAR RNA sequence with an unpaired adenosine. *J. Biomol. Struct. Dyn. 10*, 367−387.
47. Fox, K. R., and Waring, M. J. (1987) Footprinting at low temperature: evidence that ethidium and other simple intercalators can discriminate between different nucleotide sequences. *Nucleic Acids Res. 15*, 491−507.
48. Marsch, G. A., Graves, D. E., and Rill, R. L. (1995) Photoaffinity approaches to determining the sequence selectivities of DNA-small molecule interactions: actinomycin D and ethidium. *Nucleic Acids Res. 23*, 1252−1259.
49. Graves, D. E. (2001) Targetting DNA through covalent interactions of reversible binding drugs. *Methods Enzymol. 340*, 377−395.
50. Leng, F., Graves, D., and Chaires, J. B. (1998) Chemical cross-linking of ethidium to DNA by glyoxal. *Biochim. Biophys. Acta 1442*, 71−81.
51. Wang, J. C. (1974) The degree of unwinding of the DNA helix by ethidium. *J. Mol. Biol. 89*, 783−801.
52. Watkins, T. I. (1952) Trypanocides of the phenanthridine series. I. The effect of changing the quaternary grouping in dimidium bromide. *J. Chem. Soc.*, 3059−3064.
53. Mergny, J. L., Collier, D., Rougée, M., Montenay-Garestier, T., and Hélène, C. (1991) Intercalation of ethidium bromide into a triple-stranded oligonucleotide. *Nucleic Acids Res. 19*, 1521−1526.
54. Scaria, P. V., and Shafer, R. H. (1991) Binding of ethidium bromide to a DNA triple helix. Evidence for intercalation. *J. Biol. Chem. 266*, 5417−5423.
55. Sun, J. S., Lavery, R., Chomilier, J., Zakrewska, K., Montenay-Garestier, T., and Hélène, C. (1991) Theoretical study of ethidium intercalation in triple-stranded DNA and at triplex−duplex junctions. *J. Biomol. Struct. Dyn. 9*, 425−4436.
56. Tuite, E., and Norden, B. (1995) Intercalative interactions of ethidium dyes with triplex structures. *Bioorg. Med Chem. 3*, 701−711.
57. Walker, G. T., Stone, M. P., and Krugh, T. R. (1985) Ethidium binding to left-handed (Z) DNAs results in regions of right-handed DNA at the intercalation site. *Biochemistry 24*, 7462−7471.
58. Gilbert, P. L., Graves, D. E., and Chaires, J. B. (1991) Inhibition of the B to Z transition in poly(dGdC).poly(dGdC) by covalent attachment of ethidium: equilibrium studies. *Biochemistry 30*, 10925−10931.
59. White, A. S., and Draper, D. E. (1987) Single base bulges in RNA hairpins enhance ethidium binding and promote an allosteric transition. *Nucleic Acids Res. 15*, 4049−4064.
60. Nelson, J. W., and Tinoco, I., Jr. (1985) Ethidium ion binds more strongly to a DNA double helix with a bulged cytosine than to a regular double helix. *Biochemistry 24*, 6416−6421.
61. Paoletti, J., Magee, B. B., and Magee, P. T. (1976) The structure of DNA in native chromatin as determined by ethidium bromide binding. *Prog. Nucleic Acid Res. Mol. Biol. 19*, 373−377.
62. Paoletti, J., Magee, B. B., and Magee, P. T. (1977) The structure of chromatin: interaction of ethidium bromide with native and denatured chromatin. *Biochemistry 16*, 351−357.
63. Koeppel, F., Riou, J. F., Laoui, A., Mailliet, P., Arimondo, P. B., Labit, D., Petitgenet, O., Hélène, C., and Mergny, J. L. (2001) Ethidium derivatives bind to G-quartets, inhibit telomerase and act as fluorescent probes for quadruplexes. *Nucleic Acids Res. 29*, 1087−1096.
64. Rosu, F., De Pauw, E., Guittat, L., Alberti, P., Lacroix, L., Mailliet, P., Riou, J. F., and Mergny, J. L. (2003) Selective interaction of ethidium derivatives with quadruplexes: an equilibrium dialysis and electrospray ionization mass spectrometry analysis. *Biochemistry 42*, 10361−10371.
65. Ratmeyer, L., Vinayak, R., Zon, G., and Wilson, W. D. (1992) An ethidium analogue that binds with high specificity to a base-bulged duplex from the TAR RNA region of the HIV-1 genome. *J. Med. Chem. 35*, 966−968.
66. Kuhlmann, K. F., Charbeneau, N. J., and Mosher, C. W. (1978) Synthesis, DNA-binding and biological activity of a double intercalating analogue of ethidium bromide. *Nucleic Acids Res. 5*, 2629−2641.
67. Keck, M. V., and Lippard, S. J. (1992) Unwinding of supercoiled DNA by platinum-ethidium and related complexes. *J. Am. Chem. Soc. 114*, 3386−3390.
68. Koshkin, A. A., Kropachev, K. U., Mamaev, S. V., Bulychev, N. V., Lokhov, S. G., Vlassov, V. V., and Lebedev, A. V. (1994) Ethidium and azidoethidium oligonucleotide derivatives: synthesis, complementary complexe formation and sequence-specific photomodification of the single-stranded and double-stranded target oligo- and polynucleotides. *J. Mol. Recognition 7*, 177−188.
69. Peytou, V., Condom, R., Patino, N., Guedj, R., Aubertin, A. M., Gelus, N., Bailly, C., Terreux, R., and Cabrol-Bass, D. (1999) Synthesis and antiviral activity of ethidium-arginine conjugates directed against the TAR RNA of HIV-1. *J. Med. Chem. 42*, 4042−4053.
70. Carrasco, C., Haroun, M., Hellissey, P., Baldeyrou, B., Lansiaux, A., Colson, P., Houssier, C., Wilson, W. D., Giorgi-Renault, S., and Bailly, C. (2003) Design of a composite ethidium-netropsin-anilinoacridine molecule for DNA recognition. *ChemBioChem 4*, 50−61.
71. Luedtke, N. W., Liu, Q., and Tor, Y. (2003) Synthesis, photophysical properties, and nucleic acid binding of phenanthridinium derivatives based on ethidium. *Bioorg. Med. Chem. 11*, 5235−5247.
72. Olmsted, J., III, and Kearns, D. R. (1977) Mechanism of ethidium bromide fluorescence enhancement on binding to nucleic acids. *Biochemistry 16*, 3647−3654.
73. Newton, B. A. (1957) The mode of action of phenanthridines: the effect of ethidium bromide on cell division and nucleic acid synthesis. *J. Gen. Microbiol. 17*, 718−730.
74. Elliott, W. H. (1963) Effect of antimicrobial agents on deoxyribonucleic acid polymerase. *Biochem. J. 86*, 562−567.
75. Lecointe, P., Bichet, N., Fraire, C., and Paoletti, C. (1981) The hepatic metabolism of ethidium bromide to reactive mutagenic species: biochemical and structural requirements. *Biochem. Pharmacol. 30*, 601−609.
76. Boibessot, I., Turner, C. M. R., Watson, D. G., Goldie, E., Connel, G., McIntosh, A., Grant, M. H., and Skellern, G. G. (2002)

Metabolism and distribution of phenanthridine trypanocides in *Trypanosoma brucei*. *Acta tropica 84*, 219−228.
77. Houssier, C., and O'Konski, C. T. (1981) Electrooptical instrumentation systems with their data acquisiton and treatment. In *Molecular Electrooptics* (Krause, S., Ed.), pp 309−339, Plenum Publishing, New York.
78. Colson, P., Bailly, C., and Houssier, C. (1996) Electric linear dichroism as a new tool to study sequence preference in drug binding to DNA. *Biophys. Chem. 58*, 125−140.
79. Davis, T. M., and Wilson, W. D. (2000) Determination of the refractive index increments of small molecules for correction of surface plasmon resonance data. *Anal. Biochem. 284*, 348−353.
80. Davis, T. M., and Wilson, W. D. (2001) Surface plasmon resonance biosensor analysis of RNA-small molecule interactions. *Methods Enzymol. 340*, 22−51.
81. Bailly, C., Kluza, J., Martin, C., Ellis, T., and Waring, M. J. (2004) DNase I footprinting of small molecule binding sites on DNA. *Methods Mol. Biol. 288*, 319−342.
82. Stephens, C. E., Tanious, F., Kim, S., Wilson, W. D., Schell, W. A., Perfect, J. R., Franzblau, S. G., and Boykin, D. W. (2001) Diguanidino and "reversed" diamidino 2,5-diarylfurans as antimicrobial agents. *J. Med. Chem. 44*, 1741−1748.
83. Wang, L., Carrasco, C., Kumar, A., Stephens, C. E., Bailly, C., Boykin, D. W., and Wilson, W. D. (2001) Evaluation of the influence of compound structure on the stacked-dimer formation in the DNA minor groove. *Biochemistry 40*, 2511−2521.
84. Wilson, W. D., Tanious, F. A., Fernandez-Saiz, M., and Rigl, C. T. (1997) Evaluation of drug-nucleic acid interactions by thermal melting curves. *Methods Mol. Biol. 90*, 219−240.
85. Lyng, R., Rodger, A., and Norden, B. (1992) The CD of ligand-DNA systems. 2. Poly(dA-dT) B-DNA. *Biopolymers 32*, 1201−1214.
86. Rodger, A., and Norden, B. (1997) *Circular Dichroism and Linear Dichroism*; Oxford University Press: New York.
87. Wilson, W. D., Tanious, F. A., Ding, D., Kumar, A., Boykin, D. W., Colson, P., Houssier, C., and Bailly, C. (1998) Nucleic acid interactions of unfused aromatic cations: Evaluation of proposed minor-groove, major-groove and intercalation binding modes. *J. Am. Chem. Soc. 120*, 10310−10321.
88. Waring, M. J., and Bailly, C. (1994) DNA recognition by intercalators and hybrid molecules. *J. Mol. Recognition 7*, 109−122.
89. Boykin, D. W., Kumar, A., Spychala, J., Zhou, M., Lombardi, R. L., Wilson, W. D., Dykstra, C. C., Jones, S. K., Hall, J. E., Tidwell, R. R., Laughton, C., Nunn, C. M., and Neidle, S. (1995) Dicationic diarylfurans as anti-*Pneumocystis carinii* agents. *J. Med. Chem. 38*, 912−916.
90. Trent, J. O., Clark, G. R., Kumar, A., Wilson, W. D., Boykin, D. W., Hall, J. E., Tidwell, R. R., Blagburn, B. L., and Neidle, S. (1996) Targeting the minor groove of DNA: crystal structures of two complexes between furan derivatives of berenil and the DNA dodecamer d(CGCGAATTCGCG)$_2$. *J. Med. Chem. 39*, 4554−4562.
91. Laughton, C. A., Tanious, F., Nunn, C. M., Boykin, D. W., Wilson, W. D., and Neidle, S. (1996) A crystallographic and spectroscopic study of the complex between d(CGCGAATTCGCG)$_2$ and 2,5-bis(4-guanylphenyl)furan, an analogue of berenil. Structural origins of enhanced DNA-binding affinity. *Biochemistry 35*, 5655−5661.
92. Guerri, A., Simpson, I. J., and Neidle, S. (1998) Visualization of extensive water ribbons and network in a DNA minor-groove drug complex. *Nucleic Acids Res. 26*, 2873−2878.
93. Mazur, S., Tanious, F. A., Ding, D., Kumar, A., Boykin, D. W., Simpson, I. J., Neidle, S., and Wilson, W. D. (2000) A thermodynamic and structural analysis of DNA minor groove complex formation. *J. Mol. Biol. 300*, 321−337.
94. Suh, D., and Chaires, J. B. (1995) Criteria for the mode of binding of DNA binding agents. *Bioorg. Med. Chem. 3*, 723−728.
95. Stephens, C. E., Brun, R., Salem, M. M., Werbovetz, K. A., Tanious, F., Wilson, W. D., and Boykin, D. W. (2003) The activity of diguanidino and "reversed" diamidino 2,5-diarylfurans versus *Trypanosoma cruzi* and *Leishmania donovani*. *Bioorg. Med. Chem. Lett. 13*, 2065−2069.
96. Nguyen, B., Lee, M. P. H., Hamelberg, D., Joubert, A., Bailly, C., Brun, R., Neidle, S., and Wilson, W. D. (2002) Strong binding in the DNA minor groove by an aromatic diamidine with a shape that does not match the curvature of the groove. *J. Am. Chem. Soc. 124*, 13680−13681.
97. Mallena, S., Lee, M., Bailly, C., Neidle, S., Kumar, A., Boykin, D. W., and Wilson, W. D. (2004) Thiophene based diamidine forms a "super" AT binding minor groove agent. *J. Am. Chem. Soc. 126*, 13659−13669.
98. Nguyen, B., Hamelberg, D., Bailly, C., Colson, P., Brun, R., Neidle, S., and Wilson, W. D. (2004) Characterization of a novel DNA minor groove complex. *Biophys. J. 86*, 1028−1041.

BI047983N